MOIRÉ ARTIFACT PREDICTION IN A VARIABLE DATA PRINTING ENVIRONMENT

Mu Qiao and Jan P. Allebach

School of Electrical and Computer Engineering
Purdue University, West Lafayette, IN 47907-2035, USA

ABSTRACT

With the introduction of the digital press in recent years, the cost of short-run printing jobs has decreased. The "print-on-the-fly" capability of these digital presses makes it possible to compose documents based on the contents extracted from various databases. The traditional proofing method in print shops focuses on human visual inspection of one hard copy among thousands of print-outs. However, in variable data printing (VDP), each instance of the same template could use different texts, fonts, and images obtained through various capturing devices. Visual inspection of every copy is not cost efficient in the VDP environment. In this paper, we present a scheme to automatically predict the presence of moiré artifacts in the print-out before the actual printing take place. Only the images that may induce moiré artifact with respect to the targeted press will be identified and adaptive image processing can be applied to eliminate the potential artifact.

***Index Terms*—** Digital publishing, image processing, moiré artifact detection, variable data printing,

1. INTRODUCTION

The traditional offset press workflow can produce high quality long-run jobs, normally hundreds or thousands of copies all of which are identical. The print shop generates a plate for the offset press and produces many copies of the original design on the offset press using this plate. The proofing method used in traditional print shops is visual inspection based on the fact that all print-outs are copies from the same design. Comparing with the traditional offset press, the digital press eliminates the need for a plate and enables very short run jobs and "every-page-is-different" types of publication. Document template and rules are generated independently of the data and each instance of the template is generated using these composition rules and information collected from the database. This workflow is referred to as variable data printing (VDP) [1].

In the printing workflow, color separations are halftoned and imaged independently. When superimposed, the halftone screens of the primary colors may interact to generate moiré artifacts [2]. Specially designed periodic clustered-dot color screens can suppress this type of moiré artifact [3]. However, these approaches will not suppress moiré due to the interaction between the halftone screen and the image content .

In this paper, we propose a two-phase scheme that, based on the characteristics of the digital press, automatically identifies the images that could induce moiré before the actual printing take place. We will demonstrate the scheme using monochrome images. In Section 2, we derive the spectrum of the halftone image. In Section 3 and 4 we describe a method to characterize the digital press. In Section 5, we show a procedure for detecting images that may induce moiré artifacts for the digital press. Section 6 shows results of actual prints that have moiré artifacts and our detection results.

2. MOIRÉ CAUSED BY SCREENING

The spectral analysis of the discrete parameter halftoning process in this section is an extension of [4] which demonstrates that the moiré artifact is image-induced and depends on the halftone design used. The halftone process of digital image $f[m,n]$ is realized by a screening operation that can be expressed by

$$p\big[m,n;f[m,n]\big] = \begin{cases} 1 & f[m,n] \geq \sigma_{m,n} \\ 0 & \text{otherwise} \end{cases} \quad (1)$$

where $p[m,n;a]$ is the discrete dot profile which is periodic in the horizontal and vertical directions with period M. The dot profile function $p[m,n;a]$ is the binary halftone pattern for input level a. It preserves the average absorbtance level of the input a in the halftone cell $M \times M$.

The binary halftone image $h[m,n]$ obtained by screening can be written as: $h[m,n] = p\big[m,n;f[m,n]\big]$. We can show that the Fourier spectrum $H(\mu,\nu)$ of the halftone image is given by (2).

Research supported by the Hewlett-Packard Company.

$$
\begin{aligned}
H(\mu,\nu) &= \sum_{s=0}^{M-1}\sum_{t=0}^{M-1} F_{st}\big(\mu-\frac{s}{M},\nu-\frac{t}{M}\big),\\
F_{st}(\mu,\nu) &= \sum_{l}\sum_{k} P\big[s,t;f[l,k]\big]exp\big\{-j2\pi(\mu l+\nu k)\big\},\\
P[s,t;a] &= \sum_{m=0}^{M-1}\sum_{n=0}^{M-1}\frac{p[m,n;a]}{M^2}exp\big\{\frac{-j2\pi(ms+nt)}{M}\big\}.
\end{aligned}
\tag{2}
$$

$P[s,t;a]$ is the Discrete Space Fourier Transform (DSFT) of the dot profile $p[m,n;a]$ for fixed absorptance a. This equation can be regarded as a nonlinear transformation of absorptance for fixed s and t. Eq. (2) shows that the spectrum of the halftone image consists of displaced spectra of nonlinearly transformed versions $P\big[s,t;f[k,l]\big]$ of the original digital image spectrum and the period of these replicas is M. It can be shown that the non-linear transformation of the clustered screen creates frequency doubling effect that is likely to cause moiré artifacts.

3. OVERALL SYSTEM OF MOIRÉ PREDICTION

The overall moiré prediction system consists of two phases: offline characterization of the printing device and real-time spectrum analysis. In Figure 1, the press profile includes the magnitudes and angles of the moiré inducing frequencies of the targeted rendering device. The detection algorithm processes images used to compose the document to identify potential moiré. A moiré map is generated to highlight the potential artifact region in each digital image.

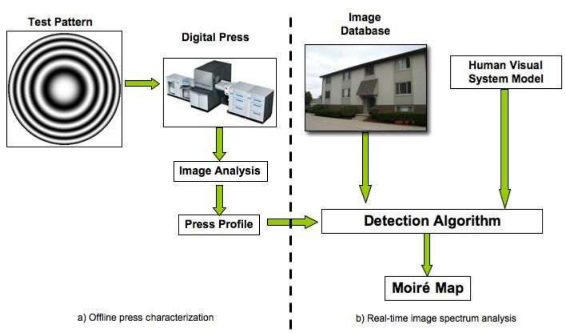

Fig. 1. Moiré prediction overall system: a) Offline press characterization, b) Real-time image spectrum analysis

4. DIGITAL PRESS CHARACTERIZATION

4.1. Test Pattern Design

We use a bullseye pattern [5] to characterize the printing device. The bullseye test pattern is a circularly symmetric sweep of an FM signal with the instantaneous frequency at each location linearly related to the distance from the center. We take the origin of the coordinate system to be the center of the test pattern, and the gray value of the pixel, whose distance to the origin is r, is described as $T[r] = A\cos\left(2\pi\, F_{MAX}\,\frac{r^2}{R}\right)$ for $r \le R/2$, where F_{MAX} is the maximum instantaneous frequency normalized with respect to sampling rate, and R is the period of the FM signal for a complete sweep of frequency from zero to F_{MAX}. The instantaneous frequency $f(r) = 2rF_{MAX}/R$ is linearly related to the distance r.

4.2. Moiré Inducing Frequency (MIF) Detection

The moiré artifact induced by the instantaneous frequency in bullseye pattern is a low frequency pattern. We define *moiré inducing frequency* (MIF) as the instantaneous frequency on the test pattern that induce artifact that does not contain high frequency component. The instantaneous frequencies near the MIF also produce moiré artifact at different frequencies and angles. The moiré artifact generated by the MIF and its neighboring frequency components form a smaller bullseye pattern as shown on Figure 2. We define this bullseye-like moiré artifact as a "secondary bullseye" in our paper and detect these "secondary bullseye" patterns to locate MIFs. Since the bullseye pattern is symmetric about the center, We only need to analyze half of the printed bullseye test page.

To detect the "secondary bullseye" pattern, we use the fact that they form concentric circles, therefore having a strong symmetry about the center of the pattern. Anisotropy is a measure of relative variance of frequency samples within a given annulus and we use anisotropy to measure the local symmetry of the scan where "secondary bullseye" exhibits high local symmetry [6].

For every pixel $B[\tilde{m},\tilde{n}]$ of the scanned bullseye pattern B, we define a region $R_{\tilde{m},\tilde{n}} = \{B[m,n] : |m-\tilde{m}| \le W, |n-\tilde{n}| \le W\}$ where $2W+1$ is the size of the region. The symmetry value of $B[\tilde{m},\tilde{n}]$ is calculated from the characteristics of $R_{\tilde{m},\tilde{n}}$. We first partition the $R_{\tilde{m},\tilde{n}}$ into N_Δ annuli with the same width Δ. All pixels in the region that belong to any one of the annuli form a set S. $S_k = \{B[m,n] : \frac{2W(k-1)}{N_\Delta} < \sqrt{(m-\tilde{m})^2+(n-\tilde{n})^2} \le \frac{2Wk}{N_\Delta}\}$ denotes the set of pixels belonging to the kth annulus from the center pixel and each annuli has $N(k)$ image pixels. For every complete annulus we compute its mean A_k and variance V_k^2

$$
A_k = \frac{1}{N(k)}\sum_{p\in S_k} p, \quad V_k^2 = \frac{1}{N(k)-1}\sum_{p\in S_k}(p-A_k)^2.
$$

The anisotropy of the kth annulus is defined as $\Psi_k = V_k^2/A_k^2$ and is a measurement of relative variance for each annulus.

The Local energy of all annuli is defined as $E = \sum_{p\in S}(p -$

$A)^2$, where $A = \sum_{p\in S} p / \sum_{k=1}^{N_\Delta} N(k)$. The local energy measurement is incorporated in calculating the symmetric measurement to eliminate misclassification of a noisy region as a region with strong symmetry. We define the symmetry value of the pixel of interest $B[\tilde{m},\tilde{n}]$ as

$$\Lambda[\tilde{m},\tilde{n}] = \sum_{k=1}^{N_\Delta} \Psi_k / E. \quad (3)$$

The higher value of Λ means stronger symmetry in the region $R_{\tilde{m},\tilde{n}}$.

The symmetry value of every pixel in the bullseye test pattern except the pixels close to the test page center is calculated to form a symmetry mask Λ. Peaks in Λ are the centers of MIFs. The MIF amplitude F and angle α can be calculated using the bullseye design parameters and the location of the peaks (4),

$$F = F_{MAX}\frac{2r}{R}, \quad \alpha = \tan^{-1}\left(\frac{y}{x}\right) \quad (4)$$

where x and y are the relative horizontal and vertical distance, respectively, from the peak to the center of the bullseye, and $r = \sqrt{x^2+y^2}$.

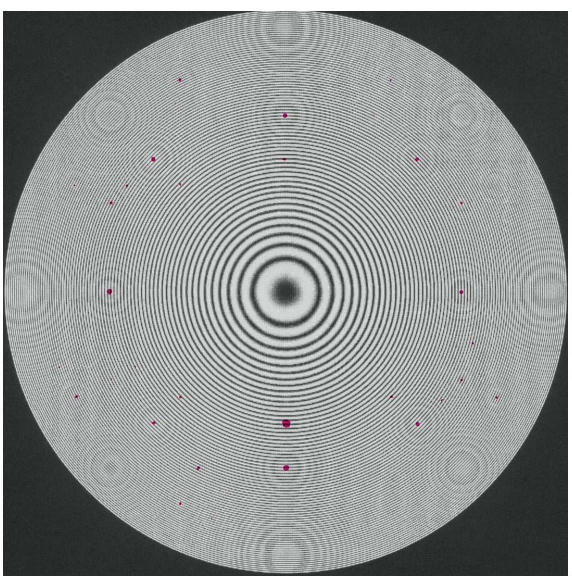

Fig. 2. MIF detected on bullseye test pattern

MIF detection results for the bullseye test pattern are shown in Figure 2. The bullseye test pattern is halftoned by a 150 cycles/inch and zero-degree screen. The red dots on the bullseye test pattern identify the MIFs found which can be mapped to frequency domain in Table 1.

Table 1. Moiré Inducing Frequencies Detected in Test Pattern

Radial frequency (cyc/inch)	Angle (degrees)
37	-90
50	-90
62	-64
53	-45
50	0
62	26
53	45
37	90
50	90

5. MIF DETECTION IN A DIGITAL IMAGE

To detect the presence of MIFs in digital images, for each pixel, we calculate the two dimensional Discrete Fourier Transform (DFT) in (5) to obtain MIF energy of a neighborhood of $N \times N$ pixels. The moiré map is generated based on the MIF energy measurement of every image pixel.

$$X[k,l] = \sum_{m=0}^{N-1}\sum_{n=0}^{N-1} x[m,n]exp\{\frac{-j2\pi(kn+lm)}{N}\} \quad (5)$$

One digital image in the image database is $\hat{m} \times \hat{n}$ pixels. Assuming the resolution is the same for both fast-scan direction and process direction [7], the image printed on the substrate is $\hat{X} \times \hat{Y}$ inches. The sampling frequency is $S = \hat{m}/\hat{X}$. Let F denote the amplitude, in cycles per inch, of the MIF that we detected in the digital press characterization and the corresponding angle of F is α. We would have the following relations for MIF horizontal and vertical components:

$$F_1 = F\cos\alpha,\ F_2 = F\sin\alpha,\ \hat{k} = [\frac{F_1 N}{S}]_R,\ \hat{l} = [\frac{F_2 N}{S}]_R$$

where $\hat{k}$ and $\hat{l}$ are the MIF's horizontal and vertical indices in the 2D DFT, respectively, and the operation $[\cdot]_R$ denotes rounding to the nearest integer.

For pixel $x[\tilde{m},\tilde{n}]$ of the digital image, its neighborhood is denoted as $h_{\tilde{m},\tilde{n}} = \{x[m,n] : |m-\tilde{m}| \le N/2, |n-\tilde{n}| \le N/2\}$. The power spectrum $P_{\tilde{m},\tilde{n}} = H_{\tilde{m},\tilde{n}}H^*_{\tilde{m},\tilde{n}}$, where $H_{\tilde{m},\tilde{m}}$ is the 2D DFT of $h_{\tilde{m},\tilde{n}}$, shows the distribution of energy at various amplitudes and angles. When a high concentration of energy is found at the MIF frequency, a moiré artifact is likely to occur.

In order to distinguish strong periodic patterns from strong edges, we compute a measure of confidence [8] that describes the relative strength of the MIF in the power spectrum. A 3×3 neighborhood of the power spectrum centered at the MIF frequency is used to calculate the confidence. The confidence $C^{\tilde{m},\tilde{n}}_{\hat{k},\hat{l}}$ is:

$$C_{\hat{k},\hat{l}}^{\tilde{m},\tilde{n}} = \left(\sum_{s=\hat{k}-1}^{\hat{k}+1} \sum_{t=\hat{l}-1}^{\hat{l}+1} P_{\tilde{m},\tilde{n}}[s,t] - P_{\tilde{m},\tilde{n}}[\hat{k},\hat{l}] \right) / P_{\tilde{m},\tilde{n}}[\hat{k},\hat{l}].$$

$M[\tilde{m},\tilde{n}]$, the moiré strength of the pixel $x[\tilde{m},\tilde{n}]$, is determined by (6).

$$M[i,j] = \begin{cases} P_{\tilde{m},\tilde{n}}[\hat{k},\hat{l}], & C_{\hat{k},\hat{l}}^{\tilde{m},\tilde{n}} \geq C_{th}, \\ 0, & \text{else.} \end{cases} \quad (6)$$

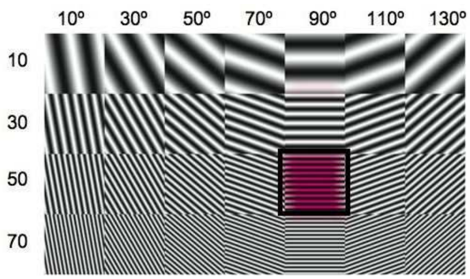

Fig. 3. Frequency of 50 cycles/inch at 90 degrees detected

Figure 3 is a digitally synthesized image consisting of sinusoidal patches whose frequency starts from 10 cycles per inch with 20 cycles per inch increment per row. The angle starts from 10 degrees on the left and increase to 130 degrees with 20 degrees increment per column. The sampling frequency is set to be 600 pixels per inch. The MIF is set at 50 cycles per inch at 90 degrees. Pixels with high MIF energy are highlighted and enclosed by a solid square on the test image.

6. RESULTS

The frequency content in the digital image interacts with the halftone profile and produces moiré that can be predicted after characterizing the printer. Figure 4 (a) is the moiré mask of 37 cycles per inch at 90 degrees. Figure 4 (b) is the print-out using a 600 dots per inch laser printer with visible moiré on the blind portion of the image, corresponding well with the moiré mask in (a) and MIF detected in Table 1. We can use the moiré mask to perform filtering operation on the selected image pixels to remove the MIFs from the digital image.

7. CONCLUSION

In this paper, we presented a scheme to automatically predict the presence of moiré artifact in the print-out before the actual printing take place. Only the images that may induce artifact with respect to the targeted printing device will be identified and adaptive image processing can be applied to eliminate the potential artifacts.

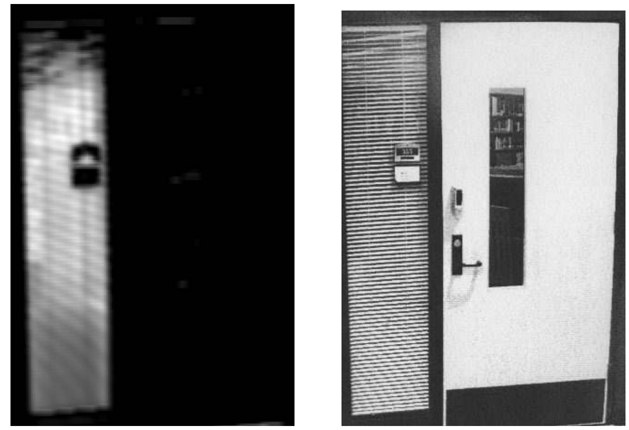

(a) **(b)**

Fig. 4. (a) Moiré mask (b) Print-out showing moiré artifact

8. REFERENCES

[1] Hewlett-Parkard Development Company, L.P. ,"HP White Paper Anvil: VDP Segmented Workflow Toolset," 2006, www.hp.com/communications.

[2] I. Amidror, R. D. Hersch, and V. Ostromoukhov, "Spectral Analysis and Minimization of Moiré Patterns in Color Separation," Journal of Electrical Imaging, vol. 3(3), pp. 295-317, July 1994.

[3] Z. He, and C. A. Bouman, "AM/FM halftoning: digital halftoning through simultaneous modulation of dot size and dot density," Journal of Electronic Imaging, vol. 13, pp. 286-302, April 2004.

[4] J. P. Allebach and B. Liu, "Analysis of halftone dot profile and aliasing in the discrete binary representation of images," Journal of Optical Society of America, vol. 67, pp. 1147-1154, 1977.

[5] T. Thong, "Digital Image Processing Test Patterns," IEEE Trans. Acoustics, Speech, and Signal Processing, vol. 31, issue 3, pp. 763-766, June 1983.

[6] R. A. Ulichney, "Dithering with Blue Noise," Proceedings of the IEEE, vol. 76, pp. 56-79, Jan. 1988.

[7] G. Sharma, Ed., *Digital Color Imaging Handbook.* CRC Press LLC, 2003, pp. 395-401

[8] A. R. Rao, and G. Thompson, "Automatic Segmentation and Descreening of Scanned Color Documents," IS&Ts NIP16: 2000 International Conference on Digital Printing Technologies, pp. 818-821, 2000